Investigation of minority carrier traps in p-type mc-Si: Effect of firing and laser annealing

Saman Jafari [*], Ziv Hameiri

The University of New South Wales, Sydney, NSW, 2052, Australia

ARTICLE INFO

ABSTRACT

Recently, it has been shown that the investigation of minority carrier traps (traps) is a useful method to study defects in silicon wafers. In this paper, we report the presence of traps in p-type multicrystalline silicon with a photoconductance decay time constant of 1.9 ± 0.4 s (at 30 °C). It is shown that the density of traps is significantly reduced after firing. However, this reduction in trap density is metastable, and it recovers by short dark annealing at 100 °C or after several days of storage at room temperature. In contrast, laser annealing is shown to eliminate the traps in fired wafers, while no change in the trap density is observed for wafers that have not been fired. Further dark annealing of those wafers does not recover the traps, suggesting that this trap annihilation is not reversible.

1. Introduction

Minority carrier traps (called "traps" hereafter) are defect centers that cause an artificially high photoconductance (PC) signal in silicon wafers [1,2]. Thus, traps can lead to artificially high lifetimes at low and medium injection levels in PC-based lifetime measurements [3]. Traps are often divided into two types: In *fast* traps, the capture and emission of a minority carrier can occur multiple times before it recombines with a majority carrier [1,3]. On the other hand, *slow* traps are considered as defect centers that effectively release the trapped minority carriers with a rate slower than the total recombination rate. Thus, the emitted carriers from *slow* traps are much more likely to recombine via other recombination channels in the sample than being re-captured by the trap [4–6].

The increase in lifetime due to traps can therefore be explained as excess majority carriers that are misinterpreted as excess minority carriers when the minority carriers are trapped [3]. The measured PC is directly correlated with the sum of the excess majority and minority carriers [7]:

$$\Delta\sigma = qw(\mu_n \Delta n + \mu_p \Delta p) \tag{1}$$

where $\Delta\sigma$ is the change in conductance, q is the elementary charge, w is the wafer's thickness, μ_n (μ_p) is the electron (hole) mobility, and Δn (Δp) is the excess carrier density in the conduction (valence) band. To calculate the excess minority carrier density from the change in PC using Eq. (1), it is assumed that the density of the excess majority and minority carriers are equal. However, in a sample impacted by trapping, the excess majority carrier concentration is equal to the sum of the excess minority carriers and the excess trapped minority carriers. Hence, the PC can be written as (for a p-type sample):

$$\Delta\sigma = qw\Delta n(\mu_n + \mu_p) + qw\Delta n_t\mu_p \tag{2}$$

where Δn_t is the change in the density of trapped carriers due to the excitation. Hence, when affected by traps, the calculated excess carrier density [Eq. (1)] is different from the actual excess carrier density and is termed as the *apparent* excess carrier density (Δn_{app}). It can be expressed using Eq. (1) assuming $\Delta n_{app} = \Delta n = \Delta p$:

$$\Delta n_{app} = \frac{\Delta\sigma}{qw(\mu_n + \mu_p)} \tag{3}$$

Combining Eqs. (2) and (3), Δn_{app} can be calculated as

$$\Delta n_{app} = \Delta n + \frac{\mu_p}{\mu_n + \mu_p}\Delta n_t \tag{4}$$

When Δn_t in Eq. (4) becomes comparable with Δn (commonly at low injection levels), the effect of traps on Δn_{app} becomes prominent and it leads to an overestimation of the actual Δn.

Traps have been observed in both mono- and multi-crystalline silicon
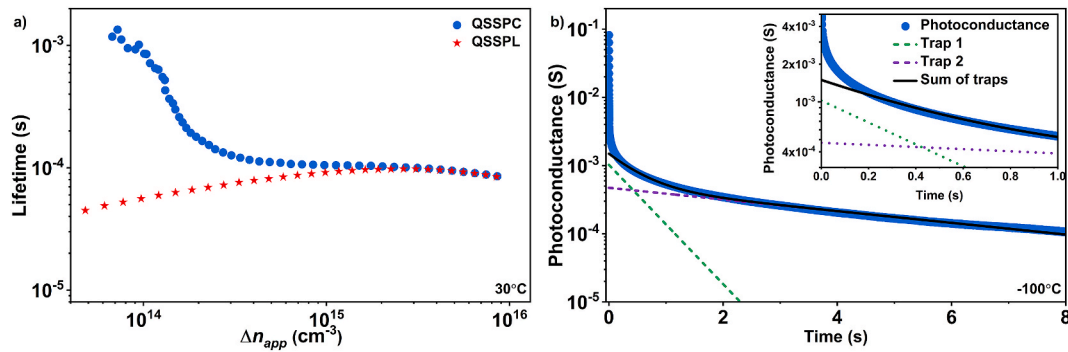
---

* Corresponding author.
E-mail address: s.jafari@student.unsw.edu.au (S. Jafari).

Fig. 1. QSSPC- and QSSPL-based lifetime (a) and photoconductance decay (b) measurements of a p-type mc-Si sample before firing. The dashed lines are the two terms of the double-exponential fit, while the solid line is their sum.

(mc-Si) wafers [2,8,9]. It has been shown that in mono-crystalline silicon, minority carrier traps can be correlated with thermal donors (in the case of both n- and p-type wafers) [5,10] and boron-oxygen (BO)-related defects (p-type wafers) [6,11]. Traps in boron-doped p-type mc-Si have been studied as well [3,8]. A study by Macdonald et al. reported the presence of *fast* traps that their density is correlated with the dislocation density [3]. Another study suggested that traps in p-type mc-Si wafers are correlated with the oxygen concentration and anticorrelated with metallic impurities [12]. It has also been shown that the traps in mc-Si wafers can be related to mobile impurities, as the density of those traps has been found to be correlated with improvement in lifetime after phosphorus-diffusion gettering [13].

It is well known that different fabrication processes have significant impacts on the quality of silicon wafers [14,15]. One of these processes is firing, which is used to form ohmic contacts between the metal grid and the silicon [16]. Moreover, the firing process releases hydrogen from hydrogen-rich dielectric layers to passivate bulk defects [17]. However, it has also been shown that firing is linked to light- and elevated temperature-induced degradation (LeTID) in mc-Si, Czochralski (Cz)- and float zone (FZ)-grown wafers [15,18,19]. To date, only a few studies have investigated the impact of fabrication processes on trap density [12,14,20]. For p-type mc-Si, it has been shown that hydrogenation through firing decreases the density of traps while post-fire annealing above 500 °C recovers them [20]. It is also shown that after gettering, while the density of traps is not reduced, they are distributed more uniformly throughout the ingot in p-type mc-Si wafers [14].

In this study, we first investigate the presence of long PCD in p-type mc-Si wafers. We demonstrate that this long PCD is due to the presence of minority carrier traps that is not related to thermal donors or BO-related traps. We then study the effect of firing, post-firing dark annealing (DA), and laser annealing on the trap densities.

2. Materials and methods

A set of p-type mc-Si wafers with a resistivity of 1.68 ± 0.05 Ω cm and thickness of 180 ± 3 μm were used in this study. Wafers were gettered via a phosphorus diffusion process at 840 °C for 45 min. The diffused layer was then removed using a hydrofluoric (HF) acid - nitric acid solution with a ratio of 1:10. Some of the samples were then passivated with silicon nitride (SiN$_x$) using a plasma-enhanced chemical vapor deposition system (refractive index of 2.08 at 632 nm) [21]. When required, the SiN$_x$ was etched off using a 5% HF solution. Firing was done using a belt furnace (SCHMID) with a wafer's peak temperature of 815 °C. For laser annealing, the samples were illuminated with a 932 nm laser at 140 °C (45 kW/m² intensity) [22].

PCD and lifetime measurements were done using our customized lifetime tester [23]. PCD measurements were performed at 30 °C before firing and at −100 °C before and after the firing process as well as after

laser annealing. PCD measurements at such a low temperature have the important benefit of a much higher signal-to-noise ratio (see Appendix A). An X5DR flash head from Quantum Instruments (identical to the flash used in the WCT-120 lifetime testers of Sinton Instruments) was used as the excitation source. The flash was used in the 1/64 mode (also known as the transient mode) with a decay time constant of around 35 μs. To determine the PCD time constants, the PCD curves were fitted using a double-exponential decay function in the form of:

$$\Delta \sigma = A_1 \left(\exp\left(-\frac{t}{\tau_1} \right) \right) + A_2 \left(\exp\left(-\frac{t}{\tau_2} \right) \right) \tag{5}$$

where A_1 and A_2 are the pre-exponential factors (correlated with the trap densities), t is the time after the flash, and τ_1 and τ_2 are the PCD time constants. Lifetime measurements were done at 30 °C before and after each PCD measurement using the same system to ensure that the measurements did not alter the lifetime. For lifetime measurements, the flash was used in the TTL mode (also known as the quasi-steady state mode) with a decay time constant of around 2.3 ms.

3. Results

3.1. Presence of trap-related long PCD time constant

Fig. 1(a) presents PC-based and photoluminescence (PL)-based lifetime measurements of a sample before firing. The two measurements well agree at high injection. However, at low injection, the PL-based lifetime decreases while the PC-based measurement significantly increases. This increase is an artifact that has been explained by the presence of traps or by the effect of depletion region modulation (DRM) [8,24]. Both have only a negligible impact on PL-based measurements [7]. Another possible explanation for the trapping effect in mc-Si wafers is a reduction of charge barrier in the vicinity of the grain boundaries due to illumination, which leads to an increase in the lateral flow of majority carriers [25–27]. However, it has been shown that the barriers return to their initial state when the illumination intensity is below 10^{-5} Suns [26,27]. Considering the maximum illumination intensity (50 Suns) and decay time constant of the flash (35 μs), illumination intensity of 10^{-6} Suns is reached ∼630 μs after the flash. As the trapping effect in this study is clearly visible for much longer times (see below), we assume that the observed effect cannot be solely explained by a change of barriers at the grain boundaries.

Fig. 1(b) shows the PCD curve of the same sample measured at −100 °C. After the excitation, there is a significant drop in the measured PC due to carrier recombination via different channels (mainly by recombination active defects). This decay is followed by a much slower second decay. Since we assume this slow decay is not due to DRM (see Appendix B), it indicates the presence of traps. The difference in the time constants of more than four orders of magnitude between the initial decay (due to carrier recombination) and the secondary decay (due to
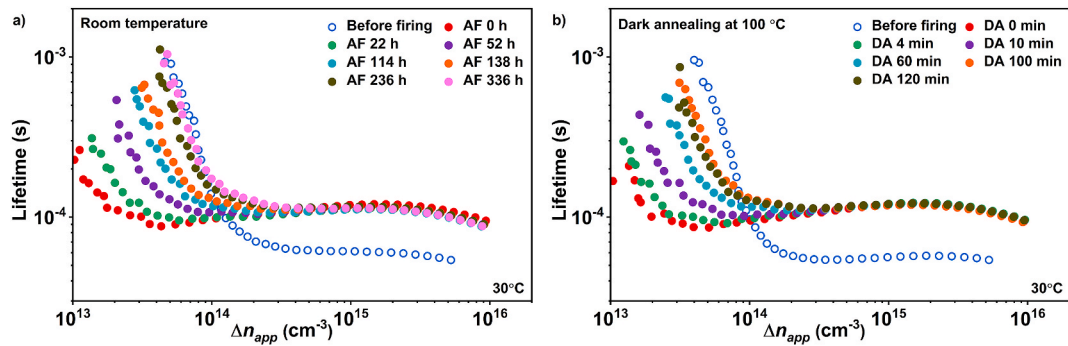
Fig. 2. QSSPC lifetime measurements of a sample before firing, after firing, and after storage at room temperature (a) and after dark annealing at 100 °C (b) for various times.

the traps) should result in a sharp transition between these two curves. However, zooming into the transition between the decays (see inset), this cannot be observed. The long decay cannot be fitted with only one exponential decay equation, suggesting that more than one trap (two trap levels or a trap with more than one energy level) is affecting the PCD curve in this range. Thus, the curve is fitted with a double-exponential decay function [Eq. (5)]. We classified the traps as *slow* traps since:

a) After removing the surface passivation (Appendix B), only a negligible change has been observed in the PCD time constants of the two traps, despite the significant drop in the lifetime. This observation indicates an insignificant re-capture of carriers after emission, suggesting that both traps are *slow* traps [2].

b) It has been shown that *slow* traps can be fitted with a "simple" exponential function, while *fast* traps cannot be fitted with such an expression [1,4]. This means that the decay rate of *slow* traps does not change with time. Since in this study, the measured PCD curves can be fitted with two time-independent constants (τ_1 and τ_2), it can be suggested that the investigated traps are *slow*.

In this study, these two traps are labeled as "Trap1" (the trap with the smaller PCD time constant) and "Trap 2" (the trap with the larger PCD time constant). The time constants for Traps 1 and 2 are determined to be 0.68 ± 0.08 s (0.14 ± 0.1 s) and 5.44 ± 0.29 s (1.87 ± 0.43 s) at -100 °C (30 °C), respectively. Since the uncertainty associated with the fitting of Trap 2 is smaller (as the fitting of the fast decay is strongly impacted by Trap 2 and might also be impacted by the effect of charge build-up around the grain boundaries [25]), in this study only the trap with the *larger* decay time constant is investigated. The long decay and the presence of traps at illumination intensity well below 10^{-5} Suns clearly indicate that barrier change around grain boundaries is not the only source of trapping in these mc-Si wafers. To the best of our knowledge, this is the first report of *slow* traps with such long decay in mc-Si, as previously observed traps in mc-Si wafers have been classified as *fast* traps [8,28]. As this trap is not due to thermal donors (see Appendix B) or BO-related traps (as will be shown below), we assume that crystallographic or/and impurity-related defects are its possible sources.

3.2. Effect of firing

Fig. 2(a) presents lifetime measurements of a sample before and after firing (labeled as "AF"). Before firing, the impact of traps is clearly noticeable at low injection. As expected, after the firing process the overall lifetime increases, probably due to improved passivation of surface and bulk defects by hydrogen that was released from the dielectric layer [17]. Interestingly, it seems that firing also has a strong impact on the trap concentration as it is significantly reduced after the process. This agrees with previous reports regarding traps in p-type
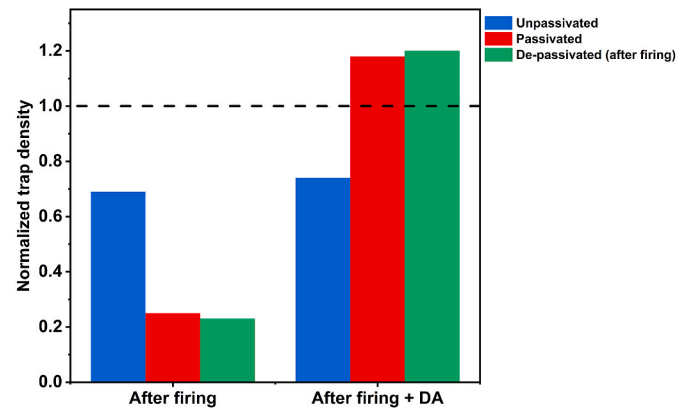

Fig. 3. Normalized trap density of unpassivated (blue), passivated (red), and samples that were de-passivated after the firing (green) after firing, and after post-firing dark annealing at 100 °C. (For interpretation of the references to colour in this figure legend, the reader is referred to the Web version of this article.)

mc-Si wafers, showing a drop in their density after firing [14,20]. However, the trap density is recovered after several days of storage at room temperature (in the dark), suggesting that the temporary low trap density is due to a metastable state.

Fig. 2(b) presents the lifetime of a second sample before and after firing, as well as after DA at 100 °C for various durations (labeled as "DA"). The same behavior is observed, in this case with a much faster recovery of the trap concentration.

Previously, Dekkers et al. reported that in order to recover annihilated traps after firing, annealing at 580 °C for 30 min is needed [20]. They indicated that the trap density is unaffected by annealing at a lower temperature (500 °C for 30 min) or without annealing. However, in this study, we observe a recovery of the trap density even at room temperature. It may be Dekkers et al. did not measure the samples for a long enough time at room temperature and therefore did not notice a change. It is also noted that they observed a change in lifetime at medium injection after annealing at 500 °C [20]. Such a change has not been observed by us. While the trap density significantly changes during DA, the lifetime at medium and high injection range demonstrates only a negligible change. It is possible that the bulk of the samples from Ref. [20] have been modified during the process, explaining both the changes in lifetime and not observing a trap recovery after the annealing process.

Fig. 3 presents the normalized trap density (NTD) of representative passivated and unpassivated samples after firing and after DA. To determine the NTD, the pre-exponential factor of the Trap 2, which is correlated with the trap density, is calculated [6]. The pre-exponents are then normalized to their initial (in here, pre-firing) values. After firing,
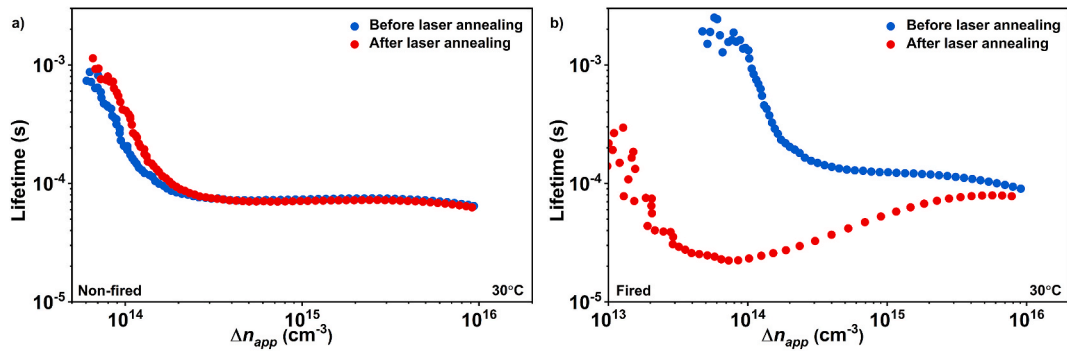
Fig. 4. QSSPC lifetime curves of non-fired (a) and fired (b) samples before and after laser annealing (45 kW/m^2 intensity) at 140 °C for 120 s.
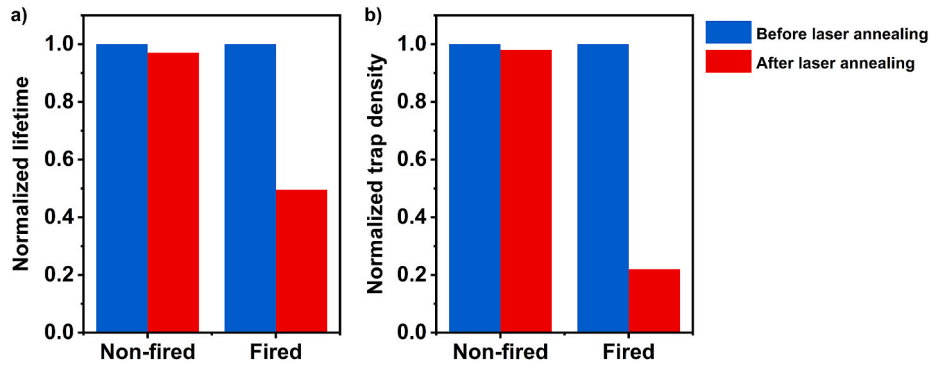

Fig. 5. Lifetime (a) and normalized trap density (b) of non-fired (blue) and fired (red) passivated samples before and after laser annealing (45 kW/m^2 intensity) at 140 °C for 120 s. (For interpretation of the references to colour in this figure legend, the reader is referred to the Web version of this article.)

the NTD of samples with surface passivation is reduced by 69 ± 3%, while for samples without passivation the reduction is much smaller, in the range of 30 ± 3%. Importantly, while the passivated samples demonstrate a full recovery after DA, the trap density of the unpassivated samples changes by less than 5%. Additional samples that have been fired *with* surface passivation, but their passivation layer *was removed* immediately after the firing (named as "de-passivated"), demonstrate similar metastable behavior as of the passivated samples. The results suggest that the metastable change in trap density after firing is related to the surface passivation. Hence, it seems that while surface passivation is required during the firing process to observe this effect, it is not needed for the recovery of the trap density. The small change in the trap density of the unpassivated samples might be due to a change in

impurities, or the removal of TDDs.

A possible explanation for this phenomenon is the interaction between complexes in the mc-Si wafer and hydrogen released from the surface passivation during firing. Initial interaction of traps with hydrogen results in passivation of the traps [20]. As a result, their density is significantly reduced immediately after firing. If the sample is kept in the dark after firing, the hydrogen presumably forms a new complex or is detached from the trap, thus the traps are re-activated and the long PCD is observed again. The PCD time constant related to the Trap 2 after the full recovery is 5.47 ± 0.28 s at −100 °C which is similar to the value before firing (5.44 ± 0.29 s). While this suggests that the source of both traps might be similar, it is not a definite conclusion, since traps with different parameters can have similar PCD time constants [2].
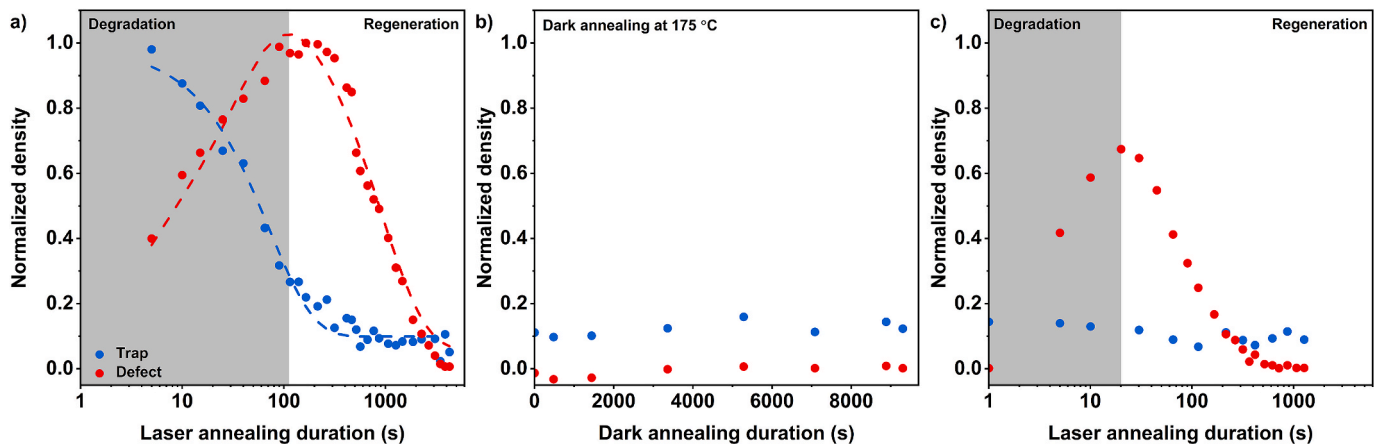

Fig. 6. Change in the normalized trap and defect densities of a passivated and fired sample after full trap recovery: after the first cycle of laser annealing (a), dark annealing (b), and after a second cycle of laser annealing (c). The dashed lines in (a) are mono- (trap) and double-exponential (defect) fits for the measurements.

3.3. Effect of laser annealing

In this section, we investigate the impact of laser annealing on the traps. Laser annealing is known to affect the lifetime of mc-Si wafers by either generating LeTID-related defects or passivating defects through hydrogenation [15,29,30].

Fig. 4 shows the change in the lifetime of non-fired and fired (after full trap recovery) samples before and after laser annealing at 140 °C for 120 s with the intensity of 45 kW/m^2. Before laser annealing, both lifetime measurements are dominated by traps at low injection. However, while the lifetime of the non-fired sample is not impacted by laser annealing, the lifetime of the fired sample has a clear reduction after laser annealing, probably due to LeTID [31]. Additionally, the trap density demonstrates a strong decrease after the laser process.

Fig. 5 presents the change in lifetime (at $0.1 \times p_0$ cm^{-3} carrier density, where p_0 is the doping density) and NTD of two representative samples (fired and non-fired) before and after laser annealing. As shown in Fig. 4, while the lifetime of the non-fired sample remains almost constant (change below 4%), the lifetime of the fired sample reduces by more than 50%. Interestingly, the NTD has the same trend, while the trap density of the non-fired sample stays almost the same after laser annealing (2% change), it demonstrates a significant reduction of almost 80% in the case of the fired sample. One possible explanation for this observation is that the traps act as a precursor of the LeTID-related defect. Thus, the laser annealing transforms the trap into a defect causing a decrease in the lifetime. To investigate this hypothesis, we measured the evolution of trap density and LeTID-related defect density during the duration of the laser annealing process.

Fig. 6 (a) demonstrates the change in NTD and normalized defect density (NDD) of a representative sample during laser annealing. Until 120 s of laser illumination, the NTD reduces while the NDD increases, demonstrating a clear anticorrelation. However, above 120 s, the NDD reduces while the NTD further decreases and then stays almost constant. Fitting the NTD with a mono-exponential decay function, a time constant of 72.7 ± 5.3 s is extracted. The NDD curve can be fitted only by using a double-exponential function to account for the simultaneous degradation and regeneration during laser annealing [32]. The calculated time constants for the defect formation and annihilation are 23.0 ± 3.5 s and 989 ± 31 s, respectively. The significantly different time constants for *trap* annihilation and *defect* formation suggests that the traps do not act as a precursor to the LeTID-related defect. Moreover, a sample that has been degraded immediately after firing, when the trap density is very low, still shows the exact same degradation rate and extent as samples that were degraded after a full trap recovery (see Appendix C). Thus, it can be concluded that while the trap annihilation might be related to the passivation of traps via hydrogenation, it is not likely to be correlated with LeTID.

Fig. 6(b) presents the change in NDD and NTD after DA of the same sample at 175 °C for 150 min. Both NDD and NTD remain almost constant throughout the annealing process. This shows that unlike post-firing DA (Fig. 3), post-laser annealing DA does not recover the traps. Hence, the trap annihilation after laser annealing seems to be irreversible. It also shows that these traps are not correlated with BO-related degradation, as BO-related traps recover after DA [6,33]. Fig. 6(c) demonstrates the change in NDD and NTD after a second cycle of laser annealing. In this cycle, the NDD has similar increasing and decreasing behavior with laser annealing duration. This change, however, happens in a shorter time scale with less degradation extent compared with the first cycle [see Fig. 6(a)]. The NTD, on the other hand, remains almost constant during the laser annealing process, different from the trends shown in the first cycle. This result further confirms that the LeTID-related defect and the observed trap are not connected, while the LeTID-related defect is recovered due to DA, the trap is not affected by this process.

4. Conclusions

A trap-related long PCD is observed in p-type mc-Si wafers. This PCD is associated with two traps with time constants of 0.14 ± 0.1 s (Trap 1) and 1.87 ± 0.43 s (Trap 2) at 30 °C. It was shown that such long time constants cannot be due to the change in the charge barrier near the grain boundaries. Additional investigations of Trap 2 indicate that firing the samples (passivated with SiN$_x$) results in a significant reduction in the density of these traps. After storing the samples at room temperature in the dark for several days or annealing the samples at 100 °C for a few hours, the traps are generated again. However, such a change is not observed in samples without surface passivation, suggesting that this metastable change in trap densities might be related to the hydrogen released from the surface passivation. It is shown that laser annealing of the fired sample permanently annihilates the traps while generates LeTID-related defect but with different rates than the trap's annihilation. Such a change is not observed in non-fired samples. It seems that there is no correlation between defect generation and trap annihilation in the case of LeTID.

CRediT authorship contribution statement

Saman Jafari: Conceptualization, Methodology, Formal analysis, Investigation, Writing – original draft. **Ziv Hameiri:** Conceptualization, Methodology, Writing – review & editing, Supervision, Funding acquisition.

Declaration of competing interest

The authors declare that they have no known competing financial interests or personal relationships that could have appeared to influence the work reported in this paper.

Acknowledgement

Appendix A. Supplementary data

Supplementary data to this article can be found online at https://doi.org/10.1016/j.solmat.2021.111341.

References

[1] J.A. Hornbeck, J.R. Haynes, Trapping of minority carriers in silicon. I. p-type silicon, Phys. Rev. 97 (1955) 311.

[2] Y. Zhu, M.K. Juhl, G. Coletti, Z. Hameiri, Reassessments of minority carrier traps in silicon with photoconductance decay measurements, IEEE J. Photovolt. 9 (2019) 652–659.

[3] D. Macdonald, A. Cuevas, Trapping of minority carriers in multicrystalline silicon, Appl. Phys. Lett. 74 (1999) 1710–1712.

[4] J. Haynes, J. Hornbeck, Trapping of minority carriers in silicon. II. n-type silicon, Phys. Rev. 100 (1955) 606.

[5] Y. Hu, H. Schøn, Ø. Nielsen, E. Johannes Øvrelid, L. Arnberg, Investigating minority carrier trapping in n-type Cz silicon by transient photoconductance measurements, J. Appl. Phys. 111 (2012), 053101.

[6] S. Jafari, Y. Zhu, F. Rougieux, J.A.T. De Guzman, V.P. Markevich, A.R. Peaker, Z. Hameiri, On the correlation between light-induced degradation and minority carrier traps in boron-doped czochralski silicon, ACS Appl. Mater. Interfaces 13 (2021) 6140–6146.

[7] R.A. Bardos, T. Trupke, M.C. Schubert, T. Roth, Trapping artifacts in quasi-steady-state photoluminescence and photoconductance lifetime measurements on silicon wafers, Appl. Phys. Lett. 88 (2006), 053504.

[8] A. Cuevas, M. Stocks, D. Macdonald, M. Kerr, C. Samundsett, Recombination and trapping in multicrystalline silicon, IEEE Trans. Electron. Dev. 46 (1999) 2026–2034.

[9] J. Schmidt, K. Bothe, R. Hezel, Oxygen-related minority-carrier trapping centers in p-type Czochralski silicon, Appl. Phys. Lett. 80 (2002) 4395–4397.

[10] M. Siriwardhana, Y. Zhu, Z. Hameiri, D. Macdonald, F. Rougieux, Photoconductance determination of carrier capture cross sections of slow traps in silicon through variable pulse filling, IEEE J. Photovolt. 11 (2021) 273–281.

[11] S. Jafari, Y. Zhu, F. Rougieux, J.A.T. De Guzman, V.P. Markevich, A.R. Peaker, Z. Hameiri, Boron-oxygen related light-induced degradation of Si solar cells: transformation between minority carrier traps and recombination active centers, in: 47th IEEE Photovoltaic Specialists Conference (PVSC), IEEE, 2020, 0689-0692.

[12] P. Gundel, M.C. Schubert, W. Warta, Origin of trapping in multicrystalline silicon, J. Appl. Phys. 104 (2008) 073716.

[13] A. Bentzen, H. Tathgar, R. Kopecek, R. Sinton, A. Holt, Recombination lifetime and trap density variations in multicrystalline silicon wafers through the block, in: 31st IEEE Photovoltaic Specialists Conference (PVSC), IEEE, 2005, pp. 1074–1077.

[14] J. Tan, A. Cuevas, D. Macdonald, T. Trupke, R. Bardos, K. Roth, On the electronic improvement of multi-crystalline silicon via gettering and hydrogenation, Prog. Photovoltaics Res. Appl. 16 (2008) 129–134.

[15] C. Vargas, K. Kim, G. Coletti, D. Payne, C. Chan, S. Wenham, Z. Hameiri, Carrier-induced degradation in multicrystalline silicon: dependence on the silicon nitride passivation layer and hydrogen released during firing, IEEE J. Photovolt. 8 (2018) 413–420.

[16] H. El Omari, J. Boyeaux, A. Laugier, Screen printed contacts formation by rapid thermal annealing in multicrystalline silicon solar cells, in: 25th IEEE Photovoltaic Specialists Conference, IEEE, 1996, pp. 585–588.

[17] J.F. Nijs, J. Szlufcik, J. Poortmans, S. Sivoththaman, R.P. Mertens, Advanced manufacturing concepts for crystalline silicon solar cells, IEEE Trans. Electron. Dev. 46 (1999) 1948–1969.

[18] D. Chen, M. Kim, B.V. Stefani, B.J. Hallam, M.D. Abbott, C.E. Chan, R. Chen, D. N. Payne, N. Nampalli, A. Ciesla, Evidence of an identical firing-activated carrier-induced defect in monocrystalline and multicrystalline silicon, Sol. Energy Mater. Sol. Cells 172 (2017) 293–300.

[19] T. Niewelt, F. Schindler, W. Kwapil, R. Eberle, J. Schön, M.C. Schubert, Understanding the light-induced degradation at elevated temperatures: similarities between multicrystalline and floatzone p-type silicon, Prog. Photovoltaics Res. Appl. 26 (2018) 533–542.

[20] H. Dekkers, L. Carnel, G. Beaucarne, Carrier trap passivation in multicrystalline Si solar cells by hydrogen from SiNₓ:H layers, Appl. Phys. Lett. 89 (2006), 013508.

[21] Z. Hameiri, N. Borojevic, L. Mai, N. Nandakumar, K. Kim, S. Winderbaum, Low-absorbing and thermally stable industrial silicon nitride films with very low surface recombination, IEEE J. Photovolt. 7 (2017) 996–1003.

[22] D. Payne, C. Chan, B. Hallam, B. Hoex, M. Abbott, S. Wenham, D. Bagnall, Acceleration and mitigation of carrier-induced degradation in p-type multi-crystalline silicon, Phys. Status Solidi Rapid Res. Lett. 10 (2016) 237–241.

[23] Y. Zhu, Z. Hameiri, Review of injection dependent charge carrier lifetime spectroscopy, Progr. Energy 3 (2021), 012001.

[24] P.J. Cousins, D.H. Neuhaus, J.E. Cotter, Experimental verification of the effect of depletion-region modulation on photoconductance lifetime measurements, J. Appl. Phys. 95 (2004) 1854–1858.

[25] R. Sinton, J. Swirhun, M. Forsyth, T. Mankad, The effects of sub-bandgap light on QSSPC measurement of lifetime and trap density: what is the cause of trapping?, in: 25th European Photovoltaic Solar Energy Conference (EUPVSEC)/5th World Conference on Photovoltaic Energy Conversion (WCPEC-5) WIP, 2010, pp. 1073–1077.

[26] C.H. Seager, Grain boundaries in polycrystalline silicon, Annu. Rev. Mater. Sci. 15 (1985) 271–302.

[27] D.P. Joshi, D.P. Bhatt, Theory of grain boundary recombination and carrier transport in polycrystalline silicon under optical illumination, IEEE Trans. Electron. Dev. 37 (1990) 237–249.

[28] D.H. Macdonald, Recombination and Trapping in Multicrystalline Silicon Solar Cells, Australian National University, 2001.

[29] B.J. Hallam, P.G. Hamer, S. Wang, L. Song, N. Nampalli, M.D. Abbott, C.E. Chan, D. Lu, A.M. Wenham, L. Mai, Advanced hydrogenation of dislocation clusters and boron-oxygen defects in silicon solar cells, Energy Procedia 77 (2015) 799–809.

[30] C. Vargas, Y. Zhu, G. Coletti, C. Chan, D. Payne, M. Jensen, Z. Hameiri, Recombination parameters of lifetime-limiting carrier-induced defects in multicrystalline silicon for solar cells, Appl. Phys. Lett. 110 (2017), 092106.

[31] M.A. Jensen, A.E. Morishige, J. Hofstetter, D.B. Needleman, T. Buonassisi, Evolution of LeTID defects in p-type multicrystalline silicon during degradation and regeneration, IEEE J. Photovolt. 7 (2017) 980–987.

[32] C. Vargas, G. Coletti, C. Chan, D. Payne, Z. Hameiri, On the impact of dark annealing and room temperature illumination on p-type multicrystalline silicon wafers, Sol. Energy Mater. Sol. Cells 189 (2019) 166–174.

[33] K. Bothe, J. Schmidt, Electronically activated boron-oxygen-related recombination centers in crystalline silicon, J. Appl. Phys. 99 (2006), 013701.